ACS OMEGA

Open Access

http://pubs.acs.org/journal/acsodf

Article

Hydrothermal Liquefaction of Organic Waste Model Compounds: The Effect of the Heating Rate on Biocrude Yield and Quality from Mixtures of Cellulose−Albumin−Sunflower Oil

Alessandro Amadei, Maria Paola Bracciale, Martina Damizia, Paolo De Filippis, Benedetta de Caprariis,* Jean-Henry Ferrasse,* and Marco Scarsella

Cite This: *ACS Omega* 2024, 9, 41194−41207

Read Online

ACCESS | Metrics & More | Article Recommendations | Supporting Information

ABSTRACT: Hydrothermal liquefaction (HTL) is a promising technology for the conversion of high-moisture biomass into a liquid biofuel precursor without predrying treatment. This study investigated the effects of the heating rate (20−110 °C/min) and feedstock composition on phase repartition of the HTL products. HTL tests were carried out using as feedstocks cellulose, egg albumin, and sunflower oil as model compounds for carbohydrates, proteins, and lipids, alone and in binary mixtures. The biocrude, solid residue, and aqueous phase were characterized in terms of composition and elemental percentage. The effects of binary interactions were studied in terms of product yields and compositions. It was observed that higher heating rates resulted in lower solid yields from all the cellulose-containing feedstocks and, in most cases, in higher biocrude yields and higher energy recovery. The results showed that the heating rate influences also the oil composition. Biocrude and solid yields were compared with their prediction based on the combination of the yields of single model compounds, showing a general increase in biocrude yields and a decrease in solid yields. The most significant deviation is observed with the mixture cellulose−albumin both for the biocrude and solid yields. In fact, the main interactions were recognized for carbohydrate−protein mixtures followed by carbohydrate−lipid and protein−lipid mixtures.

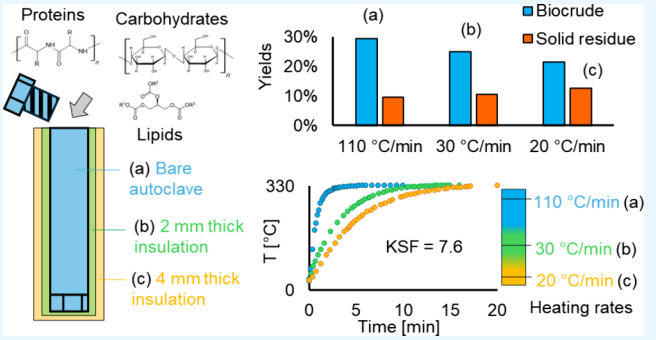

1. INTRODUCTION

The growth of global population and the expansion of emerging economies and markets have led in the past decades to a rising demand for energy and raw materials. One of the most evident and immediate consequences is the increase in waste materials derived from unsustainable production models that have led, in the spirit of developing a real circular economy, to a highly intensive R&D activity targeted to study new technologies for exploiting the today considered potential resources. Together with recycling and composting, the conversion of waste to produce energy appears to be a promising way to dispose a part of these waste materials, with the main aim of reducing the exploitation of fossil sources. Biogenic waste appears to be suitable for waste to energy (WtE) processes and represents a considerable fraction of the municipal solid waste[1] and of the municipal and industrial wastewater treatment-derived sludges.[2−4] Due to the high content of moisture (>60%), biogenic waste appears less attractive for traditional thermochemical WtE processes, as incineration, gasification, and pyrolysis, requiring energy-intensive preliminary dewatering steps.

In this context, hydrothermal liquefaction (HTL) is one of the most promising solutions to produce an advanced liquid biofuel precursor from the conversion of high-moisture organic feedstocks. The process takes place at high pressures (10−40 MPa) and medium temperatures (200−400 °C) in the presence of water near its critical state as reaction media.[5] In these conditions, water changes its properties and behaves as a good solvent and reagent.[5]

In hydrothermal conditions, several reactions occur, including depolymerization, hydrolysis, hydrodeoxygenation (HDO), and repolymerization, with some of them competing with each other.[6] Four phases are produced: a gaseous phase, an aqueous phase rich in soluble organic compounds, a biocrude, which is the target product, and a solid residue, consisting of a carbonaceous part (char) and the inorganic fraction of the starting feedstock (ashes). The yield and composition of these phases are strongly dependent on the specific biomass and on

Received: February 16, 2024
Revised: July 16, 2024
Accepted: September 19, 2024
Published: September 27, 2024

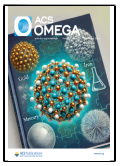

https://doi.org/10.1021/acsomega.4c01510
ACS Omega 2024, 9, 41194−41207

the operating conditions, as temperature and reaction time.[2,7−10] The chemistry behind the HTL process was investigated using model compounds, alone and in mixtures, to better define the reactions for different typologies of biomass and waste, characterized by their macro components such as carbohydrates, proteins, and lipids.[11−16]

Many of these studies are based on batch reactions and use experimental apparatuses with very different scales, ranging from large autoclaves, generally heated by electric resistances,[17] to low-volume autoclaves immersed in heated fluidized beds.[18] This results in different heating rates of the reactant mixture, with the introduction of a further variable that can strongly influence the yields and composition of the HTL products, thus hindering a straightforward comparison of all the results. While the influence of the heating rate has been largely discussed in the literature in the pyrolysis process (and is even a way to classify the different types of pyrolysis processes),[19,20] its effects on the yield and quality of the HTL products have been poorly investigated. A general increase in biocrude yields and a reduction in solid residue yields moving from low to higher heating rates are reported.[6] A correlation between the heating rate and biocrude yield from the HTL of perennial herbaceous species was studied by Zhang et al. in the range of 5−140 °C/min, demonstrating that higher heating rates enhance biocrude production.[21] Brand et al. investigated the effect of the heating rate on subcritical water HTL of sawdust and found that biocrude yields decreases for lower heating rates for the tests performed at temperatures higher than 280 °C due to the longer time in which biomass is exposed to high temperatures.[22] Tito et al.[23] also focused on the effect of the heating rate on the HTL of model compounds, reporting some interesting results about the product composition. To compare data coming from different experimental setups, some studies used as parameters empirical severity factors that integrate temperature and time.[6,10,24,25] The heating rate is not inserted in the function, such as defined by Ruyter,[26] so its effect cannot be considered and evaluated.

Due to the shortage of data on the effect of the heating rate on yields and especially on oil composition and to the importance of this parameter for a process scale-up, the aim of this work is to assess the effects of the heating rate, in the range of 20−110 °C/min, on HTL product repartition starting from organic waste model compounds, alone and in binary mixtures, focusing on the composition of the biocrude. The tests were performed in batch reactors (V = 10 mL) using cellulose, albumin, and sunflower oil as model compounds for carbohydrates, proteins, and lipids, respectively. These three classes of compounds are, in fact, the main macro components of organic materials such as sewage sludge, microalgae, and food waste.[4,10,18,27,28] Notwithstanding the evidence reported in the literature about different conditions required for the optimal conversion of these compounds,[6,9,14,29] in order to isolate the effect of the heating rate, all the other variables, such as the reactor scale, set point temperature (T = 330 °C), isothermal reaction time (t = 7 min), and biomass-to-water ratio (1:5), and procedures for product separation are kept constant.

2. MATERIALS AND METHODS

2.1. Materials. To simulate the main macro components present in organic wastes, cellulose, purchased from Sigma-Aldrich (CAS 9005-34-6), egg albumin, purchased from Dal Cin Gildo S.p.a., and edible sunflower oil were used. The inorganic content in these compounds was negligible, thus allowing direct setting of dry-ash-free mass balances for the obtained products. Acetone (CAS 67-64-1), purchased from VWR Chemicals, was used as the solvent for the biocrude extraction from the reactor.

2.2. Mixture Preparation. The three model compounds were used in pure and in their binary mixtures as dry feedstocks for HTL batch reactions. The summary of the feedstocks and their mass fraction, when combined, is reported in Table 1.

Table 1. Experimental Matrix of the Dry Mass Ratio Used for the Feedstocks

cellulose (C)	albumin (A)	sunflower oil (S)
1.00	0.00	0.00
0.75	0.25	0.00
0.50	0.50	0.00
0.25	0.75	0.00
0.00	1.00	0.00
0.75	0.00	0.25
0.50	0.00	0.50
0.25	0.00	0.75
0.00	0.00	1.00
0.00	0.75	0.25
0.00	0.50	0.50
0.00	0.25	0.75
0.00	0.00	1.00

All experiments were performed with the same reaction mixture, obtained by mixing 1 g of dry feedstock and 5 g of deionized water. For the sake of clarity, samples in the text will refer to the three letters for each compound (C, A, and S) with the mass percentage. For example, 25C-75A is the sample with 25% cellulose and 75% albumin.

2.3. HTL Reaction Setup. HTL batch reactions were carried out in stainless-steel cylindrical autoclaves with an outside diameter of 20 mm, a height of 120 mm, and an internal volume of 10 mL, for an empty total mass of about 220 g (including caps). The autoclaves were filled with 6 g of slurry and were purged with nitrogen to remove the oxygen before the reaction. Since the autoclaves were not initially pressurized, the internal pressure was self-generated by the water liquid−vapor equilibrium and by the gas and vapors produced during the reaction. The autoclaves were heated in a sand fluidized bath that was preheated to the setting temperature of 330 °C. The mixing inside the autoclaves was performed by fixing them to the shaft of a mechanical stirrer immersed in the sand bath with a rotation speed of 160 rpm. Each test was conducted in triplicate. A scheme of the reaction setup is reported in Figure 1.

The heating rate was controlled by insulating the external walls of the autoclaves adding layers of rock wool (insulating material) protected by an aluminum sheet; in order to have two heating rate values, different amounts of insulation were used. The temperature was continuously measured by a thermocouple located inside the autoclaves. In Figure 2, the temperature−time plots are shown for the three heating rates.

As the temperature plot shows, the heating rate is not constant, giving a nonlinear temperature profile when approaching the final temperature. This temperature profile is typical of a homogeneous heating of a solid by a convective heat source. The average heating rate was calculated from the heating curves measuring the time needed to reach 320 °C starting at room temperature. The maximum heating rate reached without any insulation was 110 °C/min, and the time to reach the final temperature was about 3 min. Adding insulating layers with thicknesses of about 2 and 4 mm, obtained using 0.5 and 2 g of

https://doi.org/10.1021/acsomega.4c01510
ACS Omega 2024, 9, 41194−41207

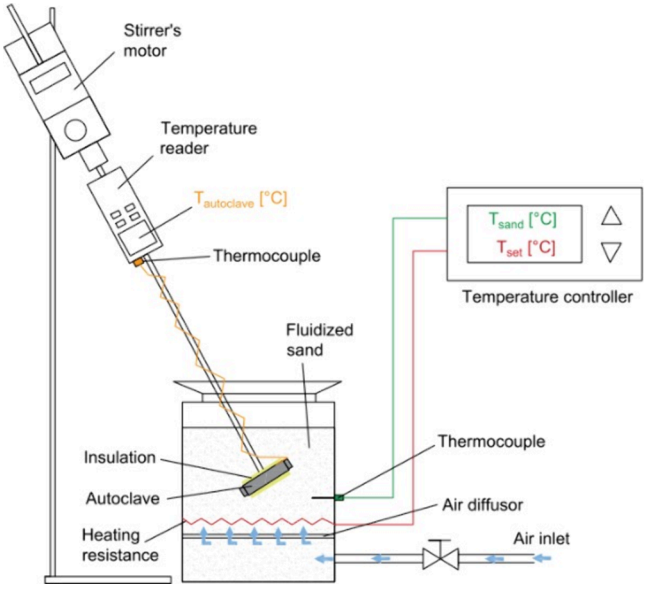

Figure 1. Scheme of the experimental setup for the HTL reactions.

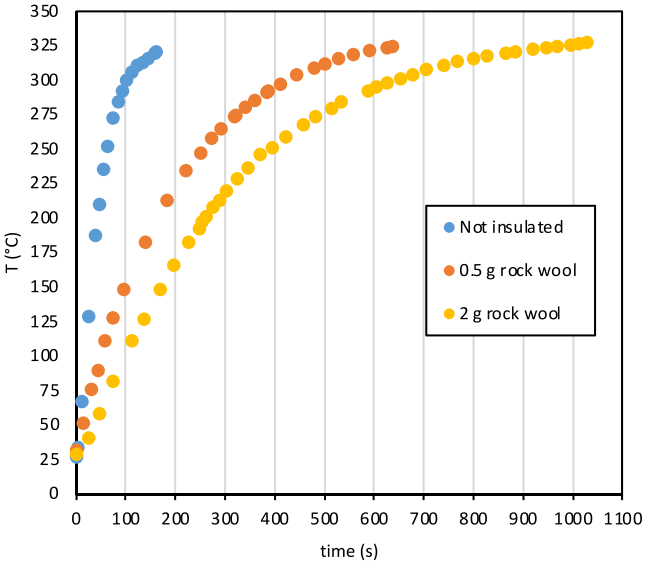

Figure 2. Autoclave's internal temperature as a function of time for the three configurations: not insulated, insulated with 0.5 g of rock wool and aluminum, and insulated with 2 g of rock wool and aluminum.

rockwool, the heating time became 9 and 13 min, corresponding to heating rates of 30 and 20 °C/min, respectively.

The residence time under isothermal conditions was maintained constant at 7 min, reaching total residence times of 10, 16, and 20 min for 110, 30, and 20 °C/min configurations, respectively. The data of the temperature profile reported in Figure 2 allow to calculate, for each configuration, a kinetic severity factor (KSF) using the same equation proposed by Tito et al.,[23] derived from a first-order kinetic model assuming a kinetic constant of 14.75 K and a reference temperature of 100 °C:

$$\mathrm{KSF} = \log_{10}\left(\int_{t_0}^{t_f} e^{T(t)-100/14.75}\,dt\right)$$

The same isothermal residence time allowed to have similar KSFs for each series of tests, respectively of 7.62, 7.59, and 7.56 for the heating rates of 110, 30, and 20 °C/min, in order to better isolate the effect of the heating rate on the experimental results.

At the end of the reaction time, the autoclaves were removed from the sand bath and quenched rapidly to room temperature using cold water to immediately freeze the ongoing reactions.

2.4. Separation of the Products and Quantification of the Yields. Once the autoclave had been cooled, it was weighed and opened removing one of the caps and left in a vertical position for 15 min to allow the evolution of the gaseous products at room temperature. Then, the degassed autoclave was weighed again, and the amount of gaseous products was measured by difference. The aqueous phase was then separated by filtration using a metallic filter cap directly mounted in the autoclave. A flow of air was blown to the other end of the autoclave to push the aqueous phase through the filter. Biocrude was extracted from the solid residue using 40 mL of acetone directly fed into the autoclave and recirculated for 10 min by a peristaltic pump. The biocrude yield was then determined gravimetrically after evaporation of the solvent at reduced pressure. The autoclave was finally left inside a ventilated oven at 80 °C overnight to dry the acetone-insoluble residue. The autoclave was then cleaned with a brush to remove the solid residue, and its amount was measured by the difference. The final weight of the reactor was compared with the initial weight of the clean reactor to ensure that no more product remained in the reactor.

2.5. Analysis of the Products. The compositions of the biocrude and aqueous phase were characterized with GC−MS analysis, performed using a 6890 model gas chromatograph with helium as the carrier gas and a mass spectroscopy detector (Agilent) using a thin-film (30 m × 0.32 mm, 0.5 μm film thickness) HP-MS5 capillary column supplied by HP. The oven temperature was programmed as follows: hold at 60 °C for 5 min, ramp at 6.5 °C/min to 265 °C, and hold at 265 °C for 3 min. The injector temperature was 250 °C, and the injector split ratio was set to 30:1. Compounds were identified by comparison of their mass spectra with those of the NIST library. Biocrude samples for GC−MS were diluted with acetone with a mass ratio of 1:5, while the aqueous phase was directly injected. Elemental analysis was carried out to investigate the elemental composition of the starting biomass, the biocrude, the solid residue, and some samples of aqueous phase. A Eurovector EA3000 elemental analyzer was used for this purpose. Complementary analyses were carried out for some samples of the solid residue and biocrude by FT-IR (Bruker Vertex 70 spectrometer; Bruker Optik GmbH) and are reported in the Supporting Information.

3. RESULTS AND DISCUSSION

3.1. Yields of the HTL Products. In Figures 3−5, the mass yields of the products are reported as a function of the feedstock composition for the various heating rates. The mass yields are calculated on a dry-ash-free basis, referred to as 1 g of dry feedstock. The yields of the gaseous phase, biocrude, and solid residue are evaluated using the formula

$$Y(\%\mathrm{d.a.f.b.}) = \frac{\text{mass of the product (g)}}{\text{mass of dry feedstock (g)}} \times 100$$

The yield of water-soluble organics, due to the possible loss of volatile compounds during separation, was not quantified experimentally and is instead evaluated by difference using the formula

https://doi.org/10.1021/acsomega.4c01510
ACS Omega 2024, 9, 41194−41207

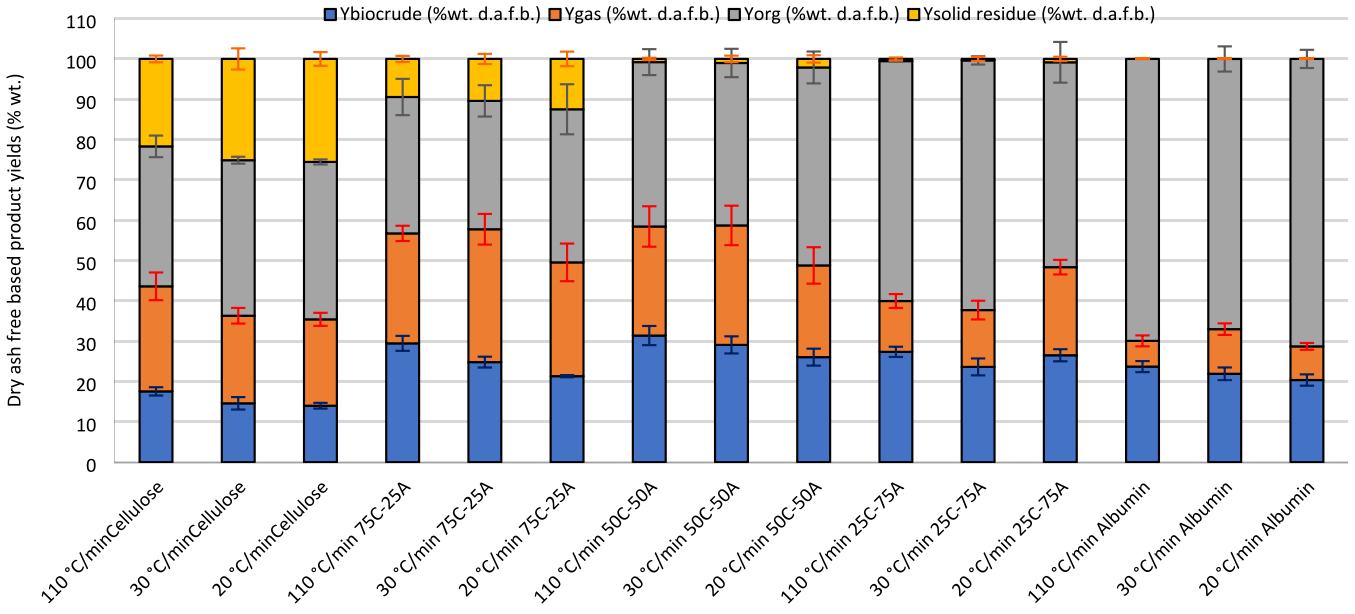

Figure 3. Dry-ash-free-based yields of the products obtained from the HTL of the cellulose−albumin mixtures for the 3 heating rates: 110, 30, and 20 °C/min.

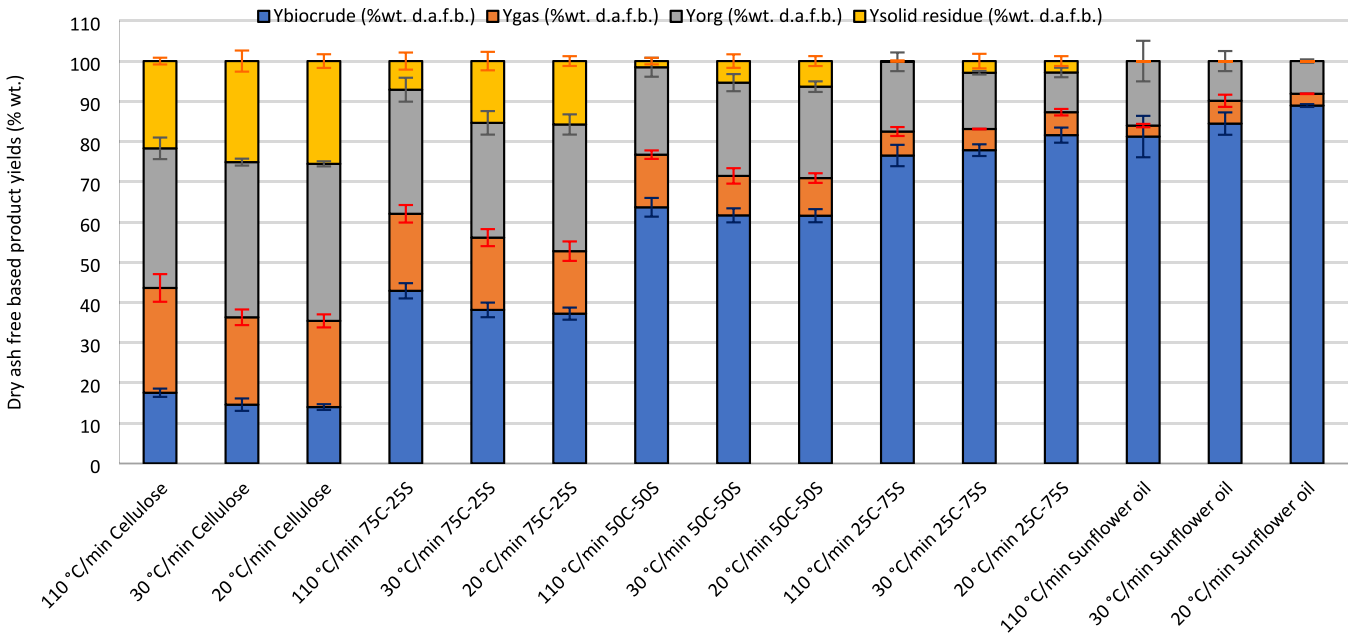

Figure 4. Dry-ash-free-based yields of the products obtained from the HTL of the cellulose−sunflower oil mixtures for the 3 heating rates: 110, 30, and 20 °C/min.

$$Y_{\text{soluble organics}}(\%\text{d.a.f.b.}) = [\text{mass of dry feedstock (g)} - \text{gaseous phase (g)} - \text{biocrude (g)} - \text{solid residue (g)}] / [\text{mass of dry feedstock (g)}] \times 100$$

The yields are presented for the main four phases that are described for HTL, gaseous, soluble organics, biocrude, and solid residue. One-way ANOVA statistical tests were conducted for each product yield in relation to the heating rates for each feedstock composition. The resulting *p*-values are presented in Table S2 of the Supporting Information.

3.1.1. Cellulose−Albumin Mixtures. Looking at Figure 3, which reports the results of the couple cellulose−albumin, it can be observed that, as expected, char is produced from the carbonization of cellulose and thus is recovered only in the tests in which cellulose is present. For all the used heating rates, the solid yield from pure cellulose is quite high, between 21.69 and 25.54 wt %. The amount of the solid residue increases with the decrease in the heating rate: a lower heating rate corresponds to a longer residence time of the reactant mixture at any temperature between room temperature and the set temperature, resulting in more time for the repolymerization reactions to take place. Consequently, the biocrude yield decreases when the heating rate is lower. This result was already observed for pure cellulose by Brand et al.,[22] reporting that fast heating rates inhibit the biocrude repolymerization for final temperatures higher than 280 °C. The amount of biocrude produced by pure cellulose is in the range of 13.99−17.55 wt %, while for pure

https://doi.org/10.1021/acsomega.4c01510
ACS Omega 2024, 9, 41194−41207

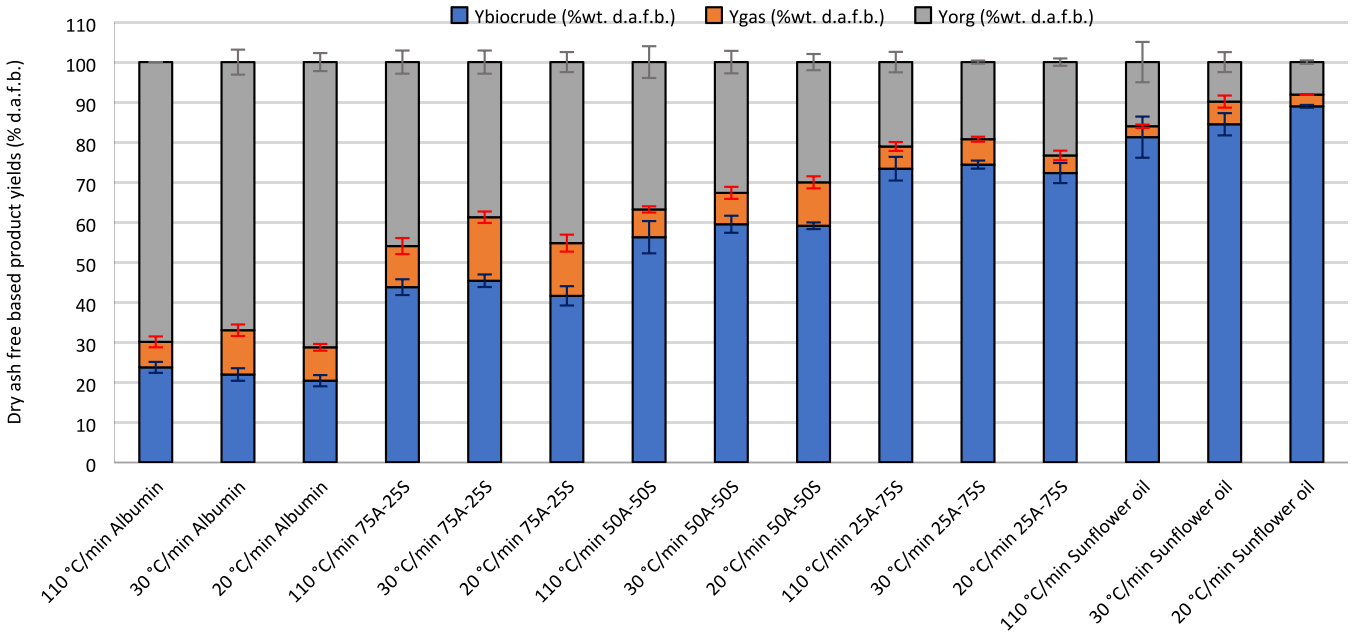

Figure 5. Dry-ash-free-based yields of the products obtained from the HTL of the albumin−sunflower oil mixtures for the 3 heating rates: 110, 30, and 20 °C/min.

albumin ranges between 20.36 and 23.69 wt %. Also, in the case of pure albumin, the biocrude amount decreases for a lower heating rate, while an increase in the gaseous products is measured. The longer residence time at middle and high temperatures, due to the longer time required for heating, can in this case promote reactions such as decarboxylation and deamination, leading to an increase in the production of volatiles and gases. The high production of soluble organics from albumin-rich feedstocks was expected due to the solubility in water of amines, amides, and other compounds derived from the degradation of amino acids.[30] The mixture of these two components causes a significant increase in the biocrude yield, with maximum values of about 26.04−31.39 wt % for the 50C-50A mixtures, higher for the higher heating rate. This increase is accompanied by a strong decrease in the solid residue yields, reaching values of 0.79−2.11 wt %, higher for the lower heating rate. The results appear consistent with the outcomes reported by Teri et al.[14] for cellulose and albumin binary mixtures for biocrude yields, which approach 31%, while the detected increase in biocrude yields and the reduction of solid yields in carbohydrates and proteins mixture, compared with the model compounds alone, confirm what was observed by Fan et al.[15] on the effects of Maillard reactions. All of the differences discussed in this section demonstrate a statistical significance greater than 90%, except for the solid residue of C50-A50 and C25-A75. For these, the yields in the solid residue are so low that statistical tests indicate a low significance when the heating rate varies.

3.1.2. Cellulose−Sunflower Oil Mixtures. In Figure 4, the results of the yields of the different products for the couple cellulose−sunflower oil as a function of the composition are reported for the three heating rates. The solid residue yield shows a trend similar to that observed for the couple cellulose−albumin, decreasing with the increase in the sunflower oil content and reaching zero for pure sunflower oil. Biocrude yields show a strong increase moving from a minimum for pure cellulose to a maximum of pure sunflower oil, that is, the feedstock that gives the highest biocrude yield. These results were expected, as sunflower oil in the adopted reaction conditions is mainly hydrolyzed to fatty acids, monoglycerides, and diglycerides, which are insoluble in water and give a high amount of an oily phase.[29] The biocrude yield obtained for the 50C-50S binary mixture, of 61.57−63.65%, appears slightly higher compared with the results obtained by Teri et al.[14] for the carbohydrate and lipid binary mixture, which approach 55%.

Because of the addition of sunflower oil, the water-soluble organic yield shows a decrease moving from pure cellulose to pure sunflower oil. Also, the yields in the gaseous phase, produced mainly by the decarboxylation reaction of cellulose decomposition, decrease moving from pure cellulose to pure sunflower oil.[31]

Comparing the yields obtained from pure sunflower oil for the three heating rates, it appears that moving from 110 to 20 °C/min, an increase in biocrude production (from 81.23 to 88.94% d.a.f.b.) and a decrease in soluble organics (from 16.03 to 8.12% d.a.f.b.) were observed, with a general decrease in the experimental error for these results. This is related to the formation of an emulsion of oil particles in the aqueous phase in the tests with higher heating rates that probably altered the measurements of both biocrude and soluble organic amounts. This effect was not observed for 20 °C/min, as for that heating rate, the total reaction time was probably sufficient for reaching higher conversions for the hydrolysis of diglycerides and monoglycerides responsible for the formation of the emulsion.[32] The temperature used appears to be too low for further degradations of fatty acids, so there are no other effects related to the reaction. The effect of the heating rate on char production from the cellulose−sunflower oil mixtures has a trend similar to that reported for cellulose−albumin mixtures, with a general increase in solid residue yields moving from 110 to 20 °C/min. All the differences that are discussed in this section show a statistical significance higher than 90%.

3.1.3. Albumin−Sunflower Oil Mixtures. The results for the couple albumin−sunflower oil are reported in Figure 5. Biocrude yields follow a trend similar to that observed for the couple cellulose-sunflower oil, showing an increase moving from pure albumin to pure sunflower oil due to the production of fatty

https://doi.org/10.1021/acsomega.4c01510
ACS Omega 2024, 9, 41194−41207

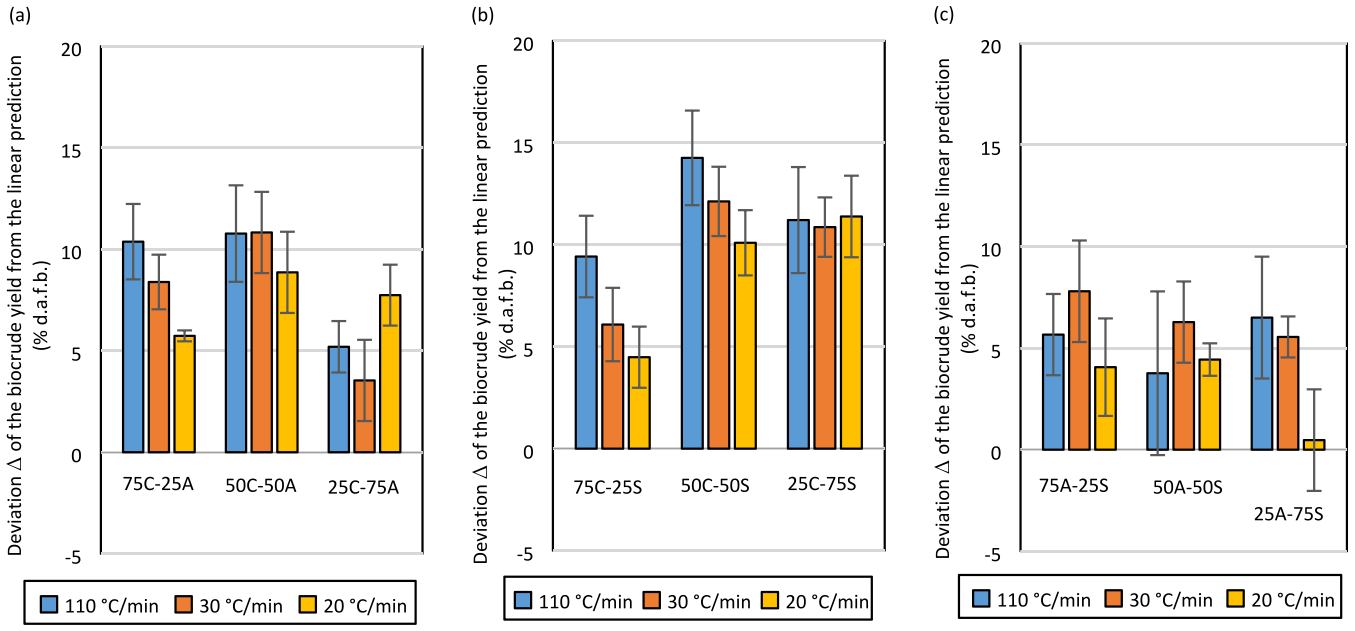

Figure 6. Deviation of the dry-ash-free-based biocrude yields from the linear prediction model for the three binary mixtures: (a) cellulose−albumin, (b) cellulose−sunflower oil, and (c) albumin−sunflower oil.

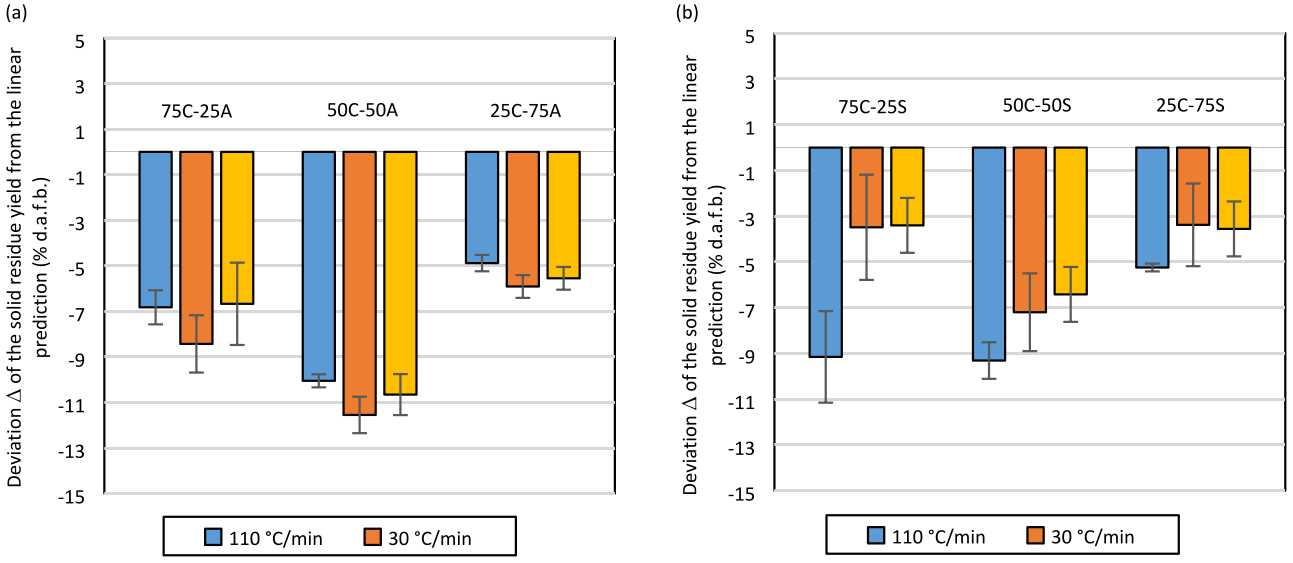

Figure 7. Deviation of the dry-ash-free-based solid residue yields from the linear prediction model for the two cellulose-containing binary mixtures: (a) cellulose−albumin and (b) cellulose−sunflower oil.

acids from the decomposition of sunflower oil. The results obtained for the 50A-50S binary mixture for biocrude yields, of 56.23−59.09%, confirm the results reported by Teri et al.,[14] approaching 60% of biocrude for protein and lipid binary mixtures. Water-soluble organic yields decrease from the maximum for pure albumin to the minimum for pure sunflower oil. When pure sunflower oil is used, in the water phase, only glycerol is detected. Both for albumin, for sunflower oil, and for their binary mixtures, the solid residue yield was zero. The product yields obtained from this binary mixture do not seem to be affected by the heating rate, as the differences observed are not significant when the heating rate varies.

3.2. Deviation of the Biocrude and Solid Residue Yields from the Linear Prediction Model. Starting from the biocrude and solid residue yields obtained from the three single model compounds, it is possible to formulate a linear prediction model for their mixtures. This simple model is generally proposed to emphasize the interaction between compounds.[33]

Based on the composition of the dry feedstock, the formula used for this modeling for each heating rate is

$$Y_{\text{linear prediction}}\ (\%\text{d. a. f. b. }) = x_C \cdot Y_C\ (\%\text{d. a. f. b. }) + x_A \cdot Y_A\ (\%\text{d. a. f. b. }) + x_S \cdot Y_S\ (\%\text{d. a. f. b. })$$

where x is the weight fraction of the single model compound in the dry feedstock (C = cellulose, A = albumin, and S = sunflower oil) and Y is the dry-ash-free-based weight percentage of the obtained product (d.a.f.b. = dry-ash-free basis).

https://doi.org/10.1021/acsomega.4c01510
ACS Omega 2024, 9, 41194−41207

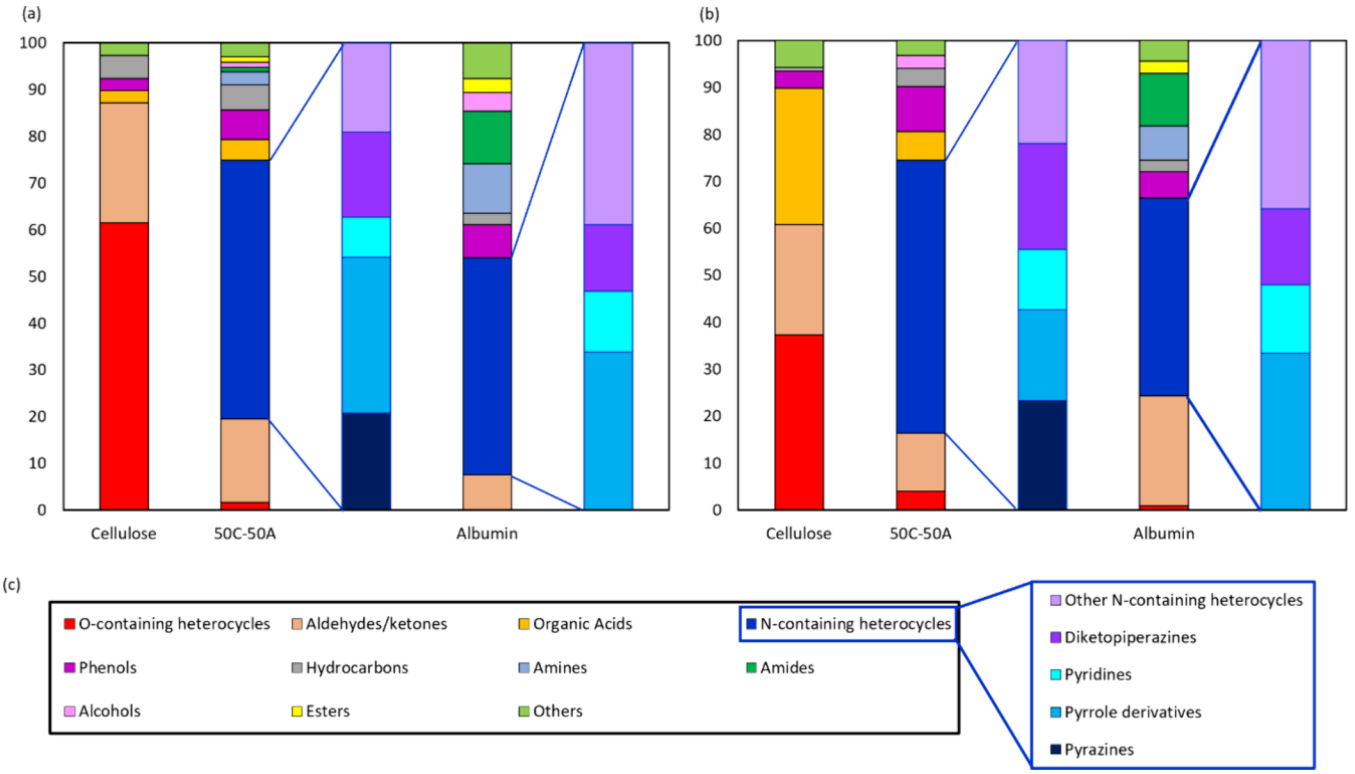

Figure 8. Composition of the biocrude obtained from the HTL of cellulose−albumin mixtures. The histograms show the area percentages of the classes of compounds detected by GC−MS analysis. Nitrogen-containing heterocycles are here divided in the subclasses of pyrazines, pyrrole derivatives, pyridines, diketopiperazines, and other N-containing heterocycles. In (a) and in (b) are reported the results for 110 and 20 °C/min, respectively. A legend is reported in (c).

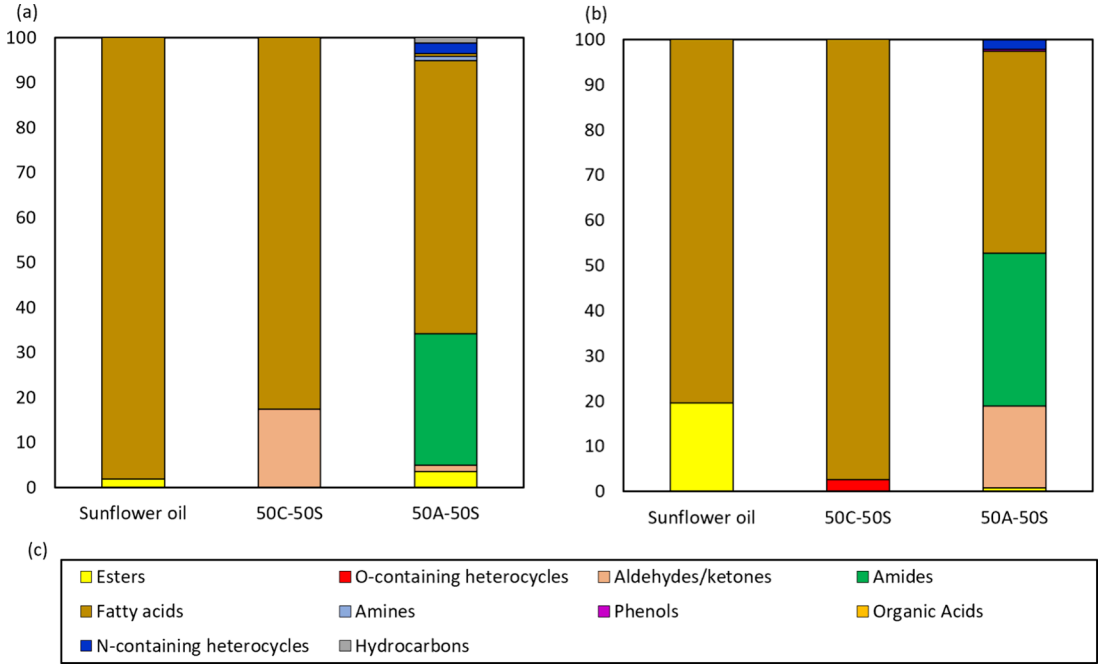

Figure 9. Composition of the biocrude obtained from the HTL of sunflower oil and its equal-percentage mixtures with cellulose and albumin. The histograms show the area percentages of the classes of compounds detected by GC−MS analysis. In (a) and in (b) are reported the results for 110 and 20 °C/min, respectively. The legend is reported in (c).

The coefficients of the model are reported for each mixture and for each heating rate in the Supporting Information (Table S2).

Using this model as reference, the plots in Figures 6 and 7 represent the deviation Δ of the obtained experimental data from the model for the biocrude yields and for the solid yields, respectively, calculated as

https://doi.org/10.1021/acsomega.4c01510
ACS Omega 2024, 9, 41194−41207

$$\Delta\ (\%\text{d. a. f. b. }) = Y_{\text{experimental}}\ (\%\text{d. a. f. b. }) - Y_{\text{linear prediction}}\ (\%\text{d. a. f. b. })$$

From Figure 6, as expected, the linear model is inadequate to predict the biocrude yield for the binary mixtures that are generally higher, especially for cellulose−albumin (Figure 6a) and cellulose−sunflower oil (Figure 6b) mixtures, for which the deviations exceed in many cases the value of 10% d.a.f.b. This result is particularly meaningful for those mixtures for which the prediction model gives lower yields, as for the cellulose−albumin mixtures ($Y_{\text{linear prediction}} \cong 15-22\%$ d.b.). The albumin−sunflower oil mixture, instead, shows a deviation from the model that has an order of magnitude similar to the experimental error and that is not so significant if reported to the experimental values of the biocrude yields.

Figure 7 shows that the linear model is also inadequate for the prediction of the solid residue yields, which are generally lower than the predicted values. The deviations of obtained experimental data from the model vary in the range of about 3−11% d.a.f.b. for both cellulose−albumin and cellulose−sunflower oil mixtures. The albumin−sunflower oil mixtures are not represented in the figure since their yields in the solid residue were zero for all the investigated mass ratios. The calculated deviations from the linear model are in some cases larger than 9% d.a.f.b. and are generally maximum for the equal-percentage mixtures, with the result of reducing considerably the solid residue yields with respect to the predicted values. While for the cellulose−sunflower oil mixtures, this reduction is generally greater when the heating is faster, cellulose−albumin mixtures show large deviations also for the slow heating rates. This trend suggests that lipids can slow down the carbohydrate's carbonization kinetics, lowering the solid residue yields as char formation requires more time to take place (see FT-IR analysis, Figure S2, of the cellulose−sunflower oil mixtures in which esters are detected also in the solid residue). Proteins may instead inhibit the carbonization reactions by subtracting the char precursors from the reaction environment in the same temperature range in which carbonization takes place. This agrees with what was reported by Fan et al.[15] about the interactions between amino acids and furan-based intermediates in Maillard reactions, forming N-containing heterocycles as pyrazines and reducing the formation of char.

The reduction of the yields in the solid residue is associated in both cases with an increase in the yields in biocrude, observed in Figure 6, as a larger part of the intermediates of the reaction are available to be converted to the product of interest.

3.3. GC−MS Analysis of Biocrude. The GC−MS-detected compounds were divided into different classes, which are reported in the Supporting Information (Table S3). The discussion reported in this section is limited to the GC-elutable part of the biocrude that was identified by the instrument and cannot be extended to its heaviest part.

Figures 8 and 9 report the compositions of the biocrude in terms of the percent area of the individuated classes. Only the results of the biocrudes obtained from the model compounds and from their equal-percentage binary mixtures for the heating rates of 110 and 20 °C/min are reported. Only the compounds that the NIST library recognizes with a quality higher than 40% were accounted for, considering the analysis of the specific fragmentation paths. The detailed tables with the whole compounds list for the biocrude and for the water-soluble organics are reported in the Supporting Information (Tables S4−S27).

The GC−MS results for the biocrudes obtained from the HTL of cellulose, albumin, and their binary mixture are reported in Figure 8. The biocrude obtained from the HTL of cellulose has a larger amount of oxygenated heterocycles, such as furfural and 2-furancarboxaldehyde,5-methyl-, a moderate amount of organic acids, including acetic acid, propanoic acid, and levulinic acid, of ketones, such as 2,5-hexanedione and 2-cyclopenten-1-one,2-hydroxy-3-methyl-, and phenols. The main detected differences between the two heating rates are resumed in a lower content of organic acids and a higher content of oxygenated heterocycles for the faster heating rate, confirming what was observed by Tito et al.[23] The absence of levulinic acid, particularly noteworthy, was observed in both the biocrude and aqueous phases at higher heating rates, whereas it emerged as one of the most abundant organic acids detected at slower heating rates. These differences are probably due to kinetic reasons, as for low heating rates, the reacting mixture stays for a longer time at each temperature lower than the set point of 330 °C. At low reaction temperatures, a retro-aldol reaction and Grob fragmentation are favored, promoting the formation of small oxygenated compounds. Instead, at higher temperatures, dehydration and decarboxylation are kinetically favored, with the formation of cyclic compounds as furan derivatives and cyclopentenes.[15]

The main compounds detected in the biocrude obtained from the HTL of albumin are N-containing heterocycles, consisting of pyrrolidine, pyrrole, piperazine, piperidine, and indole derivatives. There is then a moderate amount of ketones, as 3-penten-2-one,4-methyl-, of amides, as acetamide,*N*-(2-phenylethyl)-, and amines, as benzeneethanamine,*N*-(1-methylethylidene)-. The main differences between the two heating rates are the higher content of ketones and the lower content of amines in the biocrude obtained at the heating rate of 20 °C/min.

The results for biocrude obtained from the HTL of the equal-percentage cellulose−albumin mixture show a higher content of N-containing heterocycles compared with the results of albumin and a very low content of O-containing heterocycles compared with the results of cellulose. Furthermore, the histograms show that this is the only mixture that produces pyrazines. The results of the configuration with the slower heating rate, compared with the faster one, show a slightly higher content of N-containing heterocycles, with a higher percentage of pyrazines, pyridines, and diketopiperazines and a lower percentage of pyrrole derivatives. The other differences are summarized in a slightly higher content of phenols, organic acids, and oxygenated heterocycles and a lower content of ketones in the biocrude from the slow heating rate, compared with the faster one.

In Figure 9, the results of the GC−MS analysis of the biocrude obtained from the HTL of sunflower oil and its mixtures with cellulose and albumin are reported.

The detected compounds in the biocrude obtained from sunflower oil are fatty acids, such as *n*-hexadecanoic acid and 9,12-octadecadienoic acid, and a minor percentage of esters, mainly monoglycerides of 9,12-octadecadienoic acid, whose presence is more marked for the lower heating rate.

The biocrude obtained from the HTL of the 50C-50S mixture consists of the same fatty acids and a moderate amount of cyclic aldehydes and ketones for the fast heating rate configuration and a small amount of oxygenated heterocycles as furfural for the slow heating rate.

https://doi.org/10.1021/acsomega.4c01510
ACS Omega 2024, 9, 41194−41207

Table 2. Elemental Weight Percentages on a Dry-Ash-Free Basis of the Feedstocks and Their Obtained Biocrude and Solid Residue[b]

Reactants				
sample	N (% d.a.f.b.)	C (% d.a.f.b.)	H (% d.a.f.b.)	O[a] (% d.a.f.b.)
cellulose		44.69 ± 0.18	6.13 ± 0.03	49.18 ± 0.21
albumin	13.25 ± 0.12	47.25 ± 0.18	6.96 ± 0.23	32.37 ± 0.26
sunflower oil		74.72 ± 0.19	10.82 ± 0.60	14.46 ± 0.52
50C-50A	6.70 ± 0.04	46.07 ± 0.19	6.45 ± 0.12	40.78 ± 0.28
50C-50S		59.70 ± 0.22	8.44 ± 0.38	31.86 ± 0.60
50A-50S	6.70 ± 0.04	61.07 ± 0.17	8.76 ± 0.47	23.47 ± 0.60
Biocrude				
sample	°C/min	N (% d.a.f.b.)	C (% d.a.f.b.)	H (% d.a.f.b.)	O[a] (% d.a.f.b.)
cellulose	110		71.73 ± 0.10	5.78 ± 0.08	22.49 ± 0.18
	30		70.24 ± 0.17	4.86 ± 0.09	24.91 ± 0.18
	20		71.58 ± 0.34	5.00 ± 0.04	23.41 ± 0.36
albumin	110	8.17 ± 0.05	65.99 ± 0.46	7.75 ± 0.08	18.09 ± 0.56
	30	8.42 ± 0.11	67.16 ± 0.11	8.13 ± 0.37	16.29 ± 0.50
	20	8.64 ± 0.05	66.23 ± 0.26	8.12 ± 0.24	17.01 ± 0.35
sunflower oil	110		77.40 ± 0.15	11.17 ± 0.84	11.43 ± 0.69
	30		76.59 ± 0.66	11.99 ± 0.14	11.42 ± 0.80
	20		75.27 ± 1.01	12.18 ± 0.27	12.55 ± 1.29
50C-50A	110	7.59 ± 0.05	72.60 ± 0.42	7.69 ± 0.14	12.12 ± 0.49
	30	8.03 ± 0.11	70.27 ± 1.95	7.48 ± 0.14	14.22 ± 2.19
	20	8.33 ± 0.02	71.38 ± 0.23	7.11 ± 0.92	13.19 ± 1.13
50C-50S	110		76.74 ± 1.35	11.03 ± 0.02	12.24 ± 1.37
	30		76.74 ± 0.74	11.45 ± 0.31	11.81 ± 1.02
	20		75.92 ± 0.52	11.13 ± 0.29	12.96 ± 0.81
50A-50S	110	3.41 ± 0.06	75.12 ± 0.91	11.66 ± 0.06	9.81 ± 0.91
	30	3.39 ± 0.10	75.79 ± 0.23	11.75 ± 0.02	9.08 ± 0.29
	20	3.34 ± 0.09	75.51 ± 0.33	11.35 ± 0.30	9.79 ± 0.33
Solid residue				
sample	°C/min	N (% d.a.f.b.)	C (% d.a.f.b.)	H (% d.a.f.b.)	O[a] (% d.a.f.b.)
cellulose	110		71.04 ± 0.09	4.13 ± 0.09	24.47 ± 0.18
	30		69.26 ± 0.25	4.25 ± 0.07	26.07 ± 0.18
	20		70.03 ± 0.29	4.14 ± 0.01	25.18 ± 0.32
50C-50A	110	6.12 ± 0.11	69.28 ± 0.42	4.99 ± 0.04	19.62 ± 0.56
	30	6.42 ± 0.08	68.68 ± 1.02	5.47 ± 0.14	19.44 ± 1.23
	20	7.75 ± 0.04	67.67 ± 0.95	5.25 ± 0.20	19.32 ± 1.16
50C-50S	110		73.34 ± 2.12	4.23 ± 0.12	21.78 ± 2.25
	30		73.55 ± 0.10	4.32 ± 0.04	21.50 ± 0.17
	20		72.35 ± 0.43	4.33 ± 0.03	22.81 ± 0.44
Biocrude				
Sample	°C/min	N (% d.a.f.b.)	C (% d.a.f.b.)	H (% d.a.f.b.)	O[a] (% d.a.f.b.)
Cellulose	110	-	71.73 ± 0.10	5.78 ± 0.08	22.49 ± 0.18
	30	-	70.24 ± 0.17	4.86 ± 0.09	24.91 ± 0.18
	20	-	71.58 ± 0.34	5.00 ± 0.04	23.41 ± 0.36
Albumin	110	8.17 ± 0.05	65.99 ± 0.46	7.75 ± 0.08	18.09 ± 0.56
	30	8.42 ± 0.11	67.16 ± 0.11	8.13 ± 0.37	16.29 ± 0.50
	20	8.64 ± 0.05	66.23 ± 0.26	8.12 ± 0.24	17.01 ± 0.35
Sunflower oil	110	-	77.40 ± 0.15	11.17 ± 0.84	11.43 ± 0.69
	30	-	76.59 ± 0.66	11.99 ± 0.14	11.42 ± 0.80
	20	-	75.27 ± 1.01	12.18 ± 0.27	12.55 ± 1.29
50C − 50A	110	7.59 ± 0.05	72.60 ± 0.42	7.69 ± 0.14	12.12 ± 0.49
	30	8.03 ± 0.11	70.27 ± 1.95	7.48 ± 0.14	14.22 ± 2.19
	20	8.33 ± 0.02	71.38 ± 0.23	7.11 ± 0.92	13.19 ± 1.13
50C − 50S	110	-	76.74 ± 1.35	11.03 ± 0.02	12.24 ± 1.37
	30	-	76.74 ± 0.74	11.45 ± 0.31	11.81 ± 1.02
	20	-	75.92 ± 0.52	11.13 ± 0.29	12.96 ± 0.81
50A − 50S	110	3.41 ± 0.06	75.12 ± 0.91	11.66 ± 0.06	9.81 ± 0.91
	30	3.39 ± 0.10	75.79 ± 0.23	11.75 ± 0.02	9.08 ± 0.29
	20	3.34 ± 0.09	75.51 ± 0.33	11.35 ± 0.30	9.79 ± 0.33

https://doi.org/10.1021/acsomega.4c01510
ACS Omega 2024, 9, 41194−41207

Table 2. continued

Solid residue					
Sample	°C/min	N (% d.a.f.b.)	C (% d.a.f.b.)	H (% d.a.f.b.)	O[a] (% d.a.f.b.)
Cellulose	110	-	71.04 ± 0.09	4.13 ± 0.09	24.47 ± 0.18
	30	-	69.26 ± 0.25	4.25 ± 0.07	26.07 ± 0.18
	20	-	70.03 ± 0.29	4.14 ± 0.01	25.18 ± 0.32
50C − 50A	110	6.12 ± 0.11	69.28 ± 0.42	4.99 ± 0.04	19.62 ± 0.56
	30	6.42 ± 0.08	68.68 ± 1.02	5.47 ± 0.14	19.44 ± 1.23
	20	7.75 ± 0.04	67.67 ± 0.95	5.25 ± 0.20	19.32 ± 1.16
50C − 50S	110	-	73.34 ± 2.12	4.23 ± 0.12	21.78 ± 2.25
	30	-	73.55 ± 0.10	4.32 ± 0.04	21.50 ± 0.17
	20	-	72.35 ± 0.43	4.33 ± 0.03	22.81 ± 0.44

[a]Oxygen obtained by difference: O (% d.a.f.b.) = 100% − N (% d.a.f.b.) − C (% d.a.f.b.) − H (% d.a.f.b.). [b]C = cellulose; A = albumin; S = sunflower oil.

Table 3. Higher Heating Values (HHV) of the Starting Feedstocks and of Their Obtained Biocrudes and Energy Recovery (ER) in the Biocrudes for the Three Heating Rates

sample	$HHV_{feedstock}$ (MJ/kg)	heating rate (°C/min)	HHVbiocrude (MJ/kg)	$ER_{biocrude}$(%)
cellulose	15.08 ± 0.14	110	28.48 ± 0.18	33.15 ± 0.21
		30	26.23 ± 0.16	25.38 ± 0.15
		20	27.16 ± 0.21	25.21 ± 0.19
albumin	19.93 ± 0.39	110	30.14 ± 0.34	37.82 ± 0.43
		30	31.40 ± 0.63	36.45 ± 0.73
		20	30.94 ± 0.42	33.37 ± 0.46
sunflower oil	38.13 ± 0.92	110	40.07 ± 1.27	85.38 ± 2.71
		30	40.97 ± 0.56	90.76 ± 1.24
		20	40.59 ± 0.96	94.68 ± 2.24
50C-50A	17.51 ± 0.29	110	33.36 ± 0.36	59.83 ± 0.65
		30	31.89 ± 1.24	52.99 ± 2.06
		20	31.92 ± 1.59	47.48 ± 2.36
50C-50S	26.54 ± 0.72	110	39.50 ± 0.73	94.73 ± 1.75
		30	40.18 ± 0.85	93.34 ± 1.97
		20	39.24 ± 0.74	90.99 ± 1.72
50A-50S	28.96 ± 0.83	110	40.29 ± 0.56	78.22 ± 1.08
		30	40.77 ± 0.12	83.71 ± 0.25
		20	39.99 ± 0.48	81.59 ± 0.97

Finally, the results for the biocrude obtained from the HTL of the 50A-50S mixture still show fatty acids as the most abundant class of components followed by fatty acid derivative amides as hexadecanamide, 9-octadecenamide, and pyrrolidine,1-(1-oxo-9-octadecenyl)-. The N-containing heterocycle class is much less relevant compared with the biocrude obtained from the other albumin-containing mixtures and mainly consists of compounds that would be included in the subclass of other N-containing heterocycles.

The heating rate appears to affect the percentage of fatty acids, which is higher for the fast heating rate, and the percentages of amides and ketones, which are higher for the slow heating rate.

Most of the detected compounds were the same as, or similar to, the GC−MS compounds reported by Teri et al.[14] for HTL of mixtures of model compounds.

3.4. Elemental Analysis. The results of the elemental analysis of the model compounds, their equal-percentage binary mixtures, and the biocrude and solid residues obtained from the HTL tests are reported for the three heating rates in Table 2.

The higher heating values (HHV) of the starting feedstocks and the obtained biocrudes are calculated from the elemental percentages using the Dulong formula:[34]

$$\mathrm{HHV\ (MJ/kg)} = 0.338\cdot C + 1.428\cdot\left(H - \frac{O}{8}\right)$$

where C, H, and O are the dry-ash-free-based elemental mass percentages in the sample. From the HHV, it was possible to evaluate the percentage of energy recovery (ER) in the obtained biocrudes using the formula

$$ER_{biocrude}\ (\%) = \frac{HHV_{biocrude}\ (MJ/kg)\cdot Y_{biocrude}\ (\%d.\ a.\ f.\ b.)}{HHV_{feedstock}\ (MJ/kg)}$$

The HHV of feedstocks and biocrudes, including the ER with biocrude's production, are reported in Table 3.

The reported elemental percentages and HHV appear consistent with other data reported in the literature for similar starting feedstocks.[11,14]

Results show for all the biocrudes a decrease in the oxygen content and an increase in the carbon content compared to the starting reactants (pure or in mixtures). The most nitrogen-abundant biocrude is the one obtained from the HTL of albumin alone followed by the cellulose−albumin and albumin−sunflower oil-derived biocrudes. It is interesting to observe that the cellulose−albumin mixture and the albumin−sunflower oil mixture, which contain the same percentage of nitrogen (approximately 6.7%), give completely different results in their biocrude's nitrogen content. For the 50C-50A mixture, the

https://doi.org/10.1021/acsomega.4c01510
ACS Omega 2024, 9, 41194−41207

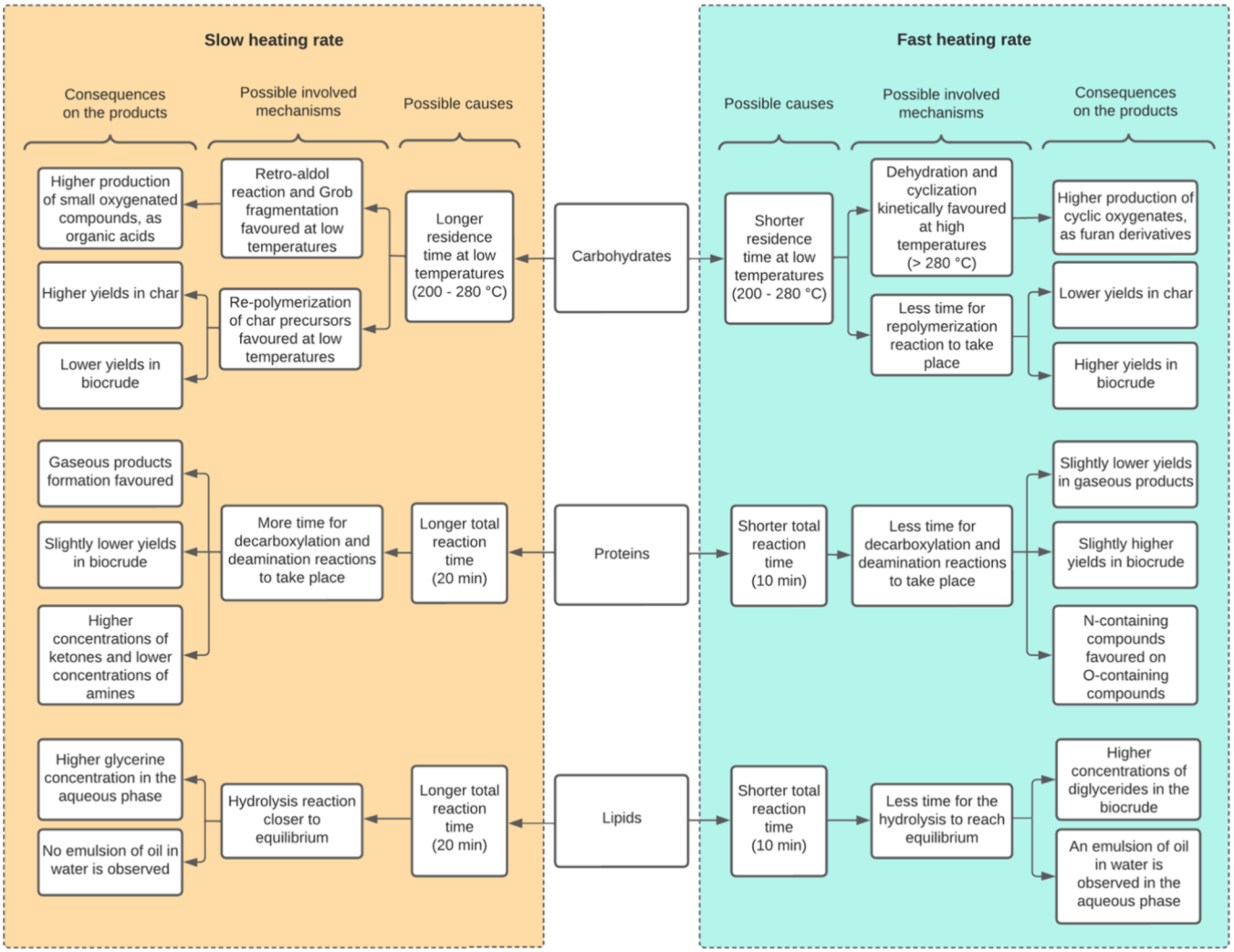

Figure 10. Summary of the effects of the heating rate on the products obtained from the HTL.

nitrogen content in the biocrude is much higher, and it is even more concentrated compared with the starting mixture. This is due to the formation of N-containing heterocycles with Maillard reactions, which fix the nitrogen in compounds as pyrazines that are less water-soluble with respect to the N-containing species produced from pure albumin, including amines as 1-butanamine and 1-pentanamine and amides as acetamide, *N*-methyl-, and propanamide,*N*-methyl-. The 50A-50S mixtures, instead, show lower percentages in nitrogen due to the presence of fatty acids, which determine higher biocrude yields and a dilution of the N-containing compounds. The nitrogen content appears to slightly increase moving from fast heating to slow heating, except for the 50A-50S mixture, which seems not to be affected by the heating rate. The results for the solid residue do not exhibit a clear trend in elemental percentages with the heating rate, except for the solid residue obtained from the HTL of the 50C-50A mixture, for which there is an increase in the nitrogen content when transitioning from fast to slow heating. This phenomenon could be attributed to the repolymerization of N-containing heterocyclic species into char, a process potentially favored by slower heating rates. Additional details, including an extended table and an elemental balance that incorporates the results of the elemental analysis of the aqueous phase, are provided in the Supporting Information (Table S28 and Figure S1). The HHV increase in the biocrudes, compared with the initial feedstocks, is particularly notable for cellulose (from 15.08 to about 26−28 MJ/kg), albumin (from 19.93 to about 30−31 MJ/kg), and their mixture (from 17.51 to about 31−33 MJ/kg). In contrast, the increase for sunflower oil is not as significant (from 38.13 to about 40 MJ/kg), owing to the resemblance between the starting feedstock and its biocrude, which is predominantly composed of fatty acids. The presence of fatty acids in the biocrude impacts the HHV of sunflower oil mixtures, approaching 40 MJ/kg for the 50C-50S and 50A-50S mixtures. The energy recovery, which incorporates both the HHV and biocrude yield, appears to decrease when transitioning from fast to slow heating, with the exception of biocrude obtained from sunflower oil and the 50A-50S mixture. While the HHV of the biocrude obtained from sunflower oil does not significantly vary with the heating rate, its yield appears to increase when moving to slow heating rates. As previously reported, this phenomenon is attributed to the oil dispersion in the aqueous phase, resulting from the formation of an oil-in-water emulsion at higher heating rates. Consequently, for faster heating rates, the oil yield appears to be lower compared to slower heating rates, directly impacting the energy recovery. The results for the ER of the biocrude obtained from the 50A-50S mixture, on the other hand, do not appear to exhibit a clear trend with the heating rate.

3.5. General Reaction Mechanisms and Comments.

The main general mechanisms involved in the hydrothermal

https://doi.org/10.1021/acsomega.4c01510
ACS Omega 2024, 9, 41194−41207

liquefaction of carbohydrates, proteins, and lipids and the effect of the heating rate on these reactions are summarized with reference to the molecules detected in the GC−MS analysis and to some reaction pathways proposed in the literature that involve those molecules.[8,11,15,16,35] The first step of the HTL process, common for all the experiments analyzed in this study, consists of the hydrolysis reactions, through which saccharides, amino acids, fatty acids, and glycerine are obtained from carbohydrates, proteins, and lipids, respectively. To reach the reaction temperature, it is obvious that a low heating rate means a longer residence time. Reactions starting at low temperatures (as hydrolysis) are then emphasized. The transformation mechanisms of these products are schematized below for each starting reactant. Some mechanisms that explain the interaction between these compounds are proposed too. The effect of the heating rate is schematized in Figure 10.

3.5.1. HTL of Carbohydrates (Cellulose). Saccharides such as glucose and fructose are produced from the hydrolysis of carbohydrates. 5-Hydroxymethyl furfural (5-HMF), 5-methyl furfural, and furfural were identified as dehydration products of fructose. Additionally, cyclic ketones such as 2-cyclopenten-1-one,2-hydroxy-3-methyl- and linear ketones such as 2,5-hexanedione were detected as further dehydration products. The presence of phenolic compounds was attributed to sugar dehydration. The presence of phenolic compounds was attributed to the dehydration of sugars, while formic acid and acetic acid were identified as byproducts of several fructose degradation steps. Levulinic acid was also recognized as a product of cleavage reactions of 5-HMF. These acids were mainly detected in the aqueous phase due to their polar nature. Decarbonylation and decarboxylation reactions can release carbon monoxide and carbon dioxide, respectively, that enrich the gaseous phase. Furthermore, cyclic oxygenated compounds as 5-HMF and levulinic acid have been identified as precursors for humin formation and hydrochar production.[35] In this study, cellulose is, in fact, the only model compound that produces solid residues under the adopted HTL conditions.

3.5.2. HTL of Proteins (Albumin). The main products of protein hydrolysis are smaller polypeptides, which can undergo further hydrolysis, and amino acids. Amines such as 1-butanamine and 1-pentanamine were identified as products of amino acid decarboxylation, while ketones such as 3-penten-2-one,4-methyl- were recognized as products of deamination and subsequent degradation of amino acids. Amides such as acetamides, propanamides, and butanamides were detected as products of amidation between acids and amines. N-containing cyclic molecules, including pyrrole, pyrrolidinone, pyrrolidinedione, and pyridine derivatives, were detected as products of amino acid cyclization, while diketopiperazines, primarily found in the aqueous phase, were identified as products of amino acid cyclodimerization. Indole and quinoline derivatives were identified as N-containing heterocycles formed through further condensation reactions.[36]

3.5.3. HTL of Lipids (Sunflower Oil). The liquefaction of triglycerides essentially consists of their hydrolysis, which produces glycerine, diglycerides, monoglycerides, and finally free fatty acids. Alenezi et al.[29] reported that the hydrolysis of the triglycerides of sunflower oil starts to happen from temperatures near 270 °C and, for the reaction temperature of 330 °C, a reaction time of 10−20 min is sufficient for the complete conversion of the triglycerides. However, the reaction times adopted in this work were not sufficient for the complete hydrolysis of diglycerides and monoglycerides. For the higher heating rates, corresponding to the shorter total reaction times, the presence of diglycerides, which cannot be detected with GC−MS analysis, led to the formation of an emulsion of oil in water. This result was not observed for the heating rate of 20 °C/min, for which the total reaction time was probably sufficient to convert most of the diglycerides. In this case, in fact, a consistent percentage of monoglycerides was detected in the biocrude, as shown in Figure 9. The fatty acid fraction appears instead to be stable under the operative conditions adopted in this study. Glycerine is entirely present in the aqueous phase due to its polar nature.

3.5.4. Interactions between Carbohydrates and Proteins (Maillard Reactions). As shown in Figure 8, mixing carbohydrates and proteins results in a strong reduction in oxygenated heterocycles and an increase in N-containing heterocycles. Also, amines and amides are reduced, if compared with the products of proteins alone, while molecules belonging to the subclass of pyrazines are produced. Pyrazines were detected and recognized in the literature (Fan et al.)[15] as one the main products of Maillard reactions, which converts saccharides and amino acids,[8,15] or their derivatives as oxygenated heterocycles and ammonia,[11,36] into N-containing heterocycles. These mechanisms consume some of the precursors for char formation, resulting in a strong reduction of solid residue yields, as shown in Figure 7a, and an increase in biocrude yields, as shown in Figure 6a. This increase in biocrude production has the side effect of increasing the nitrogen content in the biocrude, as shown in Table 2, resulting in a more difficult hydrotreating step in the following biocrude upgrading process.

3.5.5. Interactions between Carbohydrates and Lipids. GC−MS results did not show the presence of molecules clearly related to the interactions between carbohydrates and lipids. The only detected effects on the products consist in a decrease in solid residue yields and a corresponding increase in the production of acetone-soluble compounds, which was attributed to an antagonistic effect of lipids on carbonization from carbohydrate's degradation products.

3.5.6. Interactions between Proteins and Lipids. The main class of molecules directly related to the interactions between proteins and lipids consists of the amides derived from the amidation of fatty acids with ammonia, as 9-octadecenamide, with amines, as 9-octadecenamide,*N*,*N*-dimethyl-, and with N-containing heterocycles, as pyrrolidine,1-(1-oxo-9-octadecenyl)- and piperidine,1-(1-oxo-9-octadecenyl)-. This interaction is not related to a relevant effect on biocrude yields, as shown in Figure 6, as the deviations from the linear prediction model are small, if compared to the biocrude yields, and comparable with the experimental errors.

Finally, a general scheme is proposed in Figure 10 as a summary for the detected effects of the different heating rates on the HTL of carbohydrates, proteins, and lipids that were mentioned and discussed in this work.

4. CONCLUSIONS

Hydrothermal liquefaction tests were conducted at three different heating rates (20, 30, and 110 °C/min) on model compounds representing carbohydrates, proteins, and lipids, varying their ratios in binary mixtures. The study aimed to identify the main interactions between these macromolecules in relation to the heating rate. The results revealed significant interactions, leading to increased biocrude yields for all the mixtures compared to the single compounds, while solid residue yields exhibited the opposite trend when present. GC−MS

https://doi.org/10.1021/acsomega.4c01510
ACS Omega 2024, 9, 41194−41207

analysis of the 50C-50A mixture indicated a reduction in the number of O-containing heterocycles and the formation of pyrazines, products of Maillard reactions, that were recognized as the main result of the interaction between carbohydrates and proteins under the adopted conditions. Although GC−MS did not reveal specific compounds related to the cellulose−sunflower oil interaction, their effect on biocrude and solid residue yields was notable. This effect was attributed to the antagonistic effect of the lipid degradation products on the carbonization of cellulose-derived intermediates. The interaction between albumin and sunflower oil appeared less significant in terms of biocrude yields and was primarily characterized by the formation of amides from fatty acids, as detected trough GC−MS.

The main observed effect of the heating rate on product yields was its influence on repolymerization reactions in cellulose-containing mixtures, with a decrease in the solid residue yields moving from slow heating rate (20 °C/min) to fast heating rate (110 °C/min) and an increase in the biocrude yields for cellulose, from 13.99 to 17.55%, and for 50C-50A mixtures, from 26.04 to 31.40%. Consequently, an increase in the energy recovery (ER) in the biocrude with the increase in the heating rate was observed, except for pure sunflower oil and its mixture with albumin.

These results were attributed to the shorter residence time of the reactants at each temperature between room temperature and 330 °C due to the faster heating. When the heating rate is lower, in fact, some reactions can start to take place at temperatures below the set point temperature, such as the hydrolysis of diglycerides, the formation of small oxygenated compounds from carbohydrates, and the decarboxylation and deamination reactions of amino acids. These mechanisms can interfere with the characteristics of the products, altering the biocrude's composition. In the tests with cellulose and albumin for slow heating rates, higher concentrations of organic acids and a more significative production of the O-containing compounds as ketones were observed at the expense of the N-containing compounds as amines. When sunflower oil is present, the fast heating rate does not guarantee the adequate time for the completion of hydrolysis reactions, resulting in the presence of diglycerides, which are not detected for a heating rate of 20 °C/min.

These findings underscore the complexity of HTL reactions and emphasize the substantial influence of the heating rate and feedstock compositions on the products, particularly on biocrude characteristics. The heating rate emerges as a crucial factor in determining the reaction time in a continuous reactor and, consequently, reactor dimensions.

■ ASSOCIATED CONTENT

Supporting Information

The Supporting Information is available free of charge at https://pubs.acs.org/doi/10.1021/acsomega.4c01510.

Summary of the product yields; table of ANOVA statistical significance test results for the product yields; adopted linear prediction model equations for each binary mixture and heating rate; GC−MS results for the biocrude and aqueous phase; table reporting the elemental percentages for feedstocks, biocrude, solid residue, and aqueous phase; carbon and nitrogen balances; FT-IR of some biocrude and solid residue samples (PDF)

■ AUTHOR INFORMATION

Corresponding Authors

Benedetta de Caprariis − *Department of Chemical Engineering, Sapienza University of Rome, Rome 00184, Italy;* orcid.org/0000-0002-4331-9869; Email: benedetta.decaprariis@uniroma1.it

Jean-Henry Ferrasse − *Aix Marseille Univ., CNRS, Centrale Marseille, M2P2, Marseille 13453, France;* orcid.org/0000-0003-1946-7519; Email: jean-henry.ferrasse@univ-amu.fr

Authors

Alessandro Amadei − *Department of Chemical Engineering, Sapienza University of Rome, Rome 00184, Italy*

Maria Paola Bracciale − *Department of Chemical Engineering, Sapienza University of Rome, Rome 00184, Italy;* orcid.org/0000-0002-3863-1188

Martina Damizia − *Department of Chemical Engineering, Sapienza University of Rome, Rome 00184, Italy;* orcid.org/0000-0002-6953-8971

Paolo De Filippis − *Department of Chemical Engineering, Sapienza University of Rome, Rome 00184, Italy*

Marco Scarsella − *Department of Chemical Engineering, Sapienza University of Rome, Rome 00184, Italy*

Complete contact information is available at: https://pubs.acs.org/10.1021/acsomega.4c01510

Notes

The authors declare no competing financial interest.

■ REFERENCES

(1) Vergara, S. E.; Tchobanoglous, G. Municipal Solid Waste and the Environment: A Global Perspective. *Annu. Rev. Environ. Resour.* **2012**, *37* (1), 277−309.

(2) Xu, D.; Lin, G.; Liu, L.; Wang, Y.; Jing, Z.; Wang, S. Comprehensive Evaluation on Product Characteristics of Fast Hydrothermal Liquefaction of Sewage Sludge at Different Temperatures. *Energy* **2018**, *159*, 686−695.

(3) Fan, Y.; Hornung, U.; Dahmen, N. Hydrothermal Liquefaction of Sewage Sludge for Biofuel Application: A Review on Fundamentals, Current Challenges and Strategies. *Biomass Bioenergy* **2022**, *165*, No. 106570.

(4) Cabrera, D. V.; Labatut, R. A. Outlook and Challenges for Recovering Energy and Water from Complex Organic Waste Using Hydrothermal Liquefaction. *Sustain. Energy Fuels* **2021**, *5* (8), 2201−2227.

(5) Peterson, A. A.; Vogel, F.; Lachance, R. P.; Fröling, M.; Antal, M. J. Jr.; Tester, J. W. Thermochemical Biofuel Production in Hydrothermal Media: A Review of Sub- and Supercritical Water Technologies. *Energy Environ. Sci.* **2008**, *1* (1), 32.

(6) Ni, J.; Qian, L.; Wang, Y.; Zhang, B.; Gu, H.; Hu, Y.; Wang, Q. A Review on Fast Hydrothermal Liquefaction of Biomass. *Fuel* **2022**, *327*, No. 125135.

(7) Xu, C.; Lancaster, J. Conversion of Secondary Pulp/Paper Sludge Powder to Liquid Oil Products for Energy Recovery by Direct Liquefaction in Hot-Compressed Water. *Water Res.* **2008**, *42* (6−7), 1571−1582.

(8) Aierzhati, A.; Stablein, M. J.; Wu, N. E.; Kuo, C.-T.; Si, B.; Kang, X.; Zhang, Y. Experimental and Model Enhancement of Food Waste Hydrothermal Liquefaction with Combined Effects of Biochemical Composition and Reaction Conditions. *Bioresour. Technol.* **2019**, *284*, 139−147.

(9) De Caprariis, B.; De Filippis, P.; Petrullo, A.; Scarsella, M. Hydrothermal Liquefaction of Biomass: Influence of Temperature and Biomass Composition on the Bio-Oil Production. *Fuel* **2017**, *208*, 618−625.

(10) Eboibi, B. E.; Lewis, D. M.; Ashman, P. J.; Chinnasamy, S. Effect of Operating Conditions on Yield and Quality of Biocrude during Hydrothermal Liquefaction of Halophytic Microalga Tetraselmis Sp. *Bioresour. Technol.* **2014**, *170*, 20−29.
(11) Croce, A.; Battistel, E.; Chiaberge, S.; Spera, S.; De Angelis, F.; Reale, S. A Model Study to Unravel the Complexity of Bio-Oil from Organic Wastes. *ChemSusChem* **2017**, *10* (1), 171−181.
(12) Yang, J.; He, Q.; Niu, H.; Corscadden, K.; Astatkie, T. Hydrothermal Liquefaction of Biomass Model Components for Product Yield Prediction and Reaction Pathways Exploration. *Appl. Energy* **2018**, *228*, 1618−1628.
(13) Mahadevan Subramanya, S.; Savage, P. E. Identifying and Modeling Interactions between Biomass Components during Hydrothermal Liquefaction in Sub-, Near-, and Supercritical Water. *ACS Sustain. Chem. Eng.* **2021**, *9* (41), 13874−13882.
(14) Teri, G.; Luo, L.; Savage, P. E. Hydrothermal Treatment of Protein, Polysaccharide, and Lipids Alone and in Mixtures. *Energy Fuels* **2014**, *28* (12), 7501−7509.
(15) Fan, Y.; Hornung, U.; Dahmen, N.; Kruse, A. Hydrothermal Liquefaction of Protein-Containing Biomass: Study of Model Compounds for Maillard Reactions. *Biomass Convers. Biorefinery* **2018**, *8* (4), 909−923.
(16) Qiu, Y.; Aierzhati, A.; Cheng, J.; Guo, H.; Yang, W.; Zhang, Y. Biocrude Oil Production through the Maillard Reaction between Leucine and Glucose during Hydrothermal Liquefaction. *Energy Fuels* **2019**, *33* (9), 8758−8765.
(17) Song, H.; Yang, T.; Li, B.; Tong, Y.; Li, R. Hydrothermal Liquefaction of Sewage Sludge into Biocrude: Effect of Aqueous Phase Recycling on Energy Recovery and Pollution Mitigation. *Water Res.* **2022**, *226*, No. 119278.
(18) Shah, A. A.; Toor, S. S.; Conti, F.; Nielsen, A. H.; Rosendahl, L. A. Hydrothermal Liquefaction of High Ash Containing Sewage Sludge at Sub and Supercritical Conditions. *Biomass Bioenergy* **2020**, *135*, No. 105504.
(19) Debdoubi, A.; El Amarti, A.; Colacio, E.; Blesa, M. J.; Hajjaj, L. H. The Effect of Heating Rate on Yields and Compositions of Oil Products from Esparto Pyrolysis. *Int. J. Energy Res.* **2006**, *30* (15), 1243−1250.
(20) Kan, T.; Strezov, V.; Evans, T. J. Lignocellulosic Biomass Pyrolysis: A Review of Product Properties and Effects of Pyrolysis Parameters. *Renew. Sustain. Energy Rev.* **2016**, *57*, 1126−1140.
(21) Zhang, B.; Von Keitz, M.; Valentas, K. Thermochemical Liquefaction of High-Diversity Grassland Perennials. *J. Anal. Appl. Pyrolysis* **2009**, *84* (1), 18−24.
(22) Brand, S.; Hardi, F.; Kim, J.; Suh, D. J. Effect of Heating Rate on Biomass Liquefaction: Differences between Subcritical Water and Supercritical Ethanol. *Energy* **2014**, *68*, 420−427.
(23) Tito, E.; Marcolongo, C. A.; Pipitone, G.; Monteverde, A. H. A.; Bensaid, S.; Pirone, R. Understanding the Effect of Heating Rate on Hydrothermal Liquefaction: A Comprehensive Investigation from Model Compounds to a Real Food Waste. *Bioresour. Technol.* **2024**, *396*, No. 130446.
(24) Bensaid, S.; Conti, R.; Fino, D. Direct Liquefaction of Ligno-Cellulosic Residues for Liquid Fuel Production. *Fuel* **2012**, *94*, 324−332.
(25) Yanagida, T.; Fujimoto, S.; Minowa, T. Application of the Severity Parameter for Predicting Viscosity during Hydrothermal Processing of Dewatered Sewage Sludge for a Commercial PFBC Plant. *Bioresour. Technol.* **2010**, *101* (6), 2043−2045.
(26) Ruyter, H. P. Coalification Model. *Fuel* **1982**, *61* (12), 1182−1187.
(27) Maag, A.; Paulsen, A.; Amundsen, T.; Yelvington, P.; Tompsett, G.; Timko, M. Catalytic Hydrothermal Liquefaction of Food Waste Using CeZrOx. *Energies* **2018**, *11* (3), 564.
(28) Alibardi, L.; Cossu, R. Composition Variability of the Organic Fraction of Municipal Solid Waste and Effects on Hydrogen and Methane Production Potentials. *Waste Manag.* **2015**, *36*, 147−155.
(29) Alenezi, R.; Leeke, G. A.; Santos, R. C. D.; Khan, A. R. Hydrolysis Kinetics of Sunflower Oil under Subcritical Water Conditions. *Chem. Eng. Res. Des.* **2009**, *87* (6), 867−873.
(30) Sheehan, J. D.; Savage, P. E. Molecular and Lumped Products from Hydrothermal Liquefaction of Bovine Serum Albumin. *ACS Sustain. Chem. Eng.* **2017**, *5* (11), 10967−10975.
(31) Do Couto Fraga, A.; De Almeida, M. B. B.; Sousa-Aguiar, E. F. Hydrothermal Liquefaction of Cellulose and Lignin: A New Approach on the Investigation of Chemical Reaction Networks. *Cellulose* **2021**, *28* (4), 2003−2020.
(32) Loi, C. C.; Eyres, G. T.; Birch, E. J. Effect of Mono- and Diglycerides on Physical Properties and Stability of a Protein-Stabilised Oil-in-Water Emulsion. *J. Food Eng.* **2019**, *240*, 56−64.
(33) Sheng, L.; Wang, X.; Yang, X. Prediction Model of Biocrude Yield and Nitrogen Heterocyclic Compounds Analysis by Hydrothermal Liquefaction of Microalgae with Model Compounds. *Bioresour. Technol.* **2018**, *247*, 14−20.
(34) Brown, T. M.; Duan, P.; Savage, P. E. Hydrothermal Liquefaction and Gasification of Nannochloropsis Sp. *Energy Fuels* **2010**, *24* (6), 3639−3646.
(35) Chacón-Parra, A. D.; Hall, P. A.; Lewis, D. M.; Glasius, M.; Van Eyk, P. J. Elucidating the Maillard Reaction Mechanism in the Hydrothermal Liquefaction of Binary Model Compound Mixtures and Spirulina. *ACS Sustain. Chem. Eng.* **2022**, *10* (33), 10989−11003.
(36) Gai, C.; Zhang, Y.; Chen, W.-T.; Zhang, P.; Dong, Y. An Investigation of Reaction Pathways of Hydrothermal Liquefaction Using Chlorella Pyrenoidosa and Spirulina Platensis. *Energy Convers. Manag.* **2015**, *96*, 330−339.

https://doi.org/10.1021/acsomega.4c01510
ACS Omega 2024, 9, 41194−41207